Propagation of EM Fields through a Rotating Circular Hollow Dielectric Cylinder: Numerical Simulation in 2Ds

Mingtsu Ho, Hui-Hung Lin, and Tsaoan Chang
Graduate School of Opto-Mechatronics and Materials, WuFeng University, Taiwan

Abstract— The propagation of electromagnetic (EM) fields through a rotating circular hollow lossless dielectric cylinder has been numerically simulated in two dimensions and the numerical results were presented in this paper. The method of characteristics (MOC) is used to numerically solve the time-domain Maxwell equations. The passing center swing back grids (PCSBG) technique was devised and introduced in collaboration of MOC in a modified O-type grid system. The PCSBG scheme resolves the difficulty of the distortion of grid cells caused by the rotational movement of the object. There are two types of cylinder were used in this work. They are made of dielectric and impedance matching materials, illuminated by Gaussian EM pulses as the excitation sources, and may either be at rest or rotate at extremely high angular frequencies for better observation of its effects on the EM fields. The presented computational results, demonstrated in a side-by-side manner for clear comparisons, are the electric field distribution over the whole numerical domain and the EM fields sampled at the center of cylinder.

1. INTRODUCTION

The purpose of the present study is to numerically simulate the propagation of EM pulse through a rotating circular hollow dielectric cylinder and observe the effects of the rotating vessel on the EM fields. The MOC approach is used to solve the time-domain Maxwell equations in conjunction with the PCSBG technique in the modified O-type grid system. The former is for the difficulty of grid deformation caused by the rotating object while the latter for the satisfaction the requirement of minimum number of points representing the highest frequency content of interest. MOC has been reported to produce compatible results when compared with either that of finite-difference time-domain (FDTD) [1] where infinite long PEC strip was illuminated Gaussian EM pulse or theoretical values [2, 3] where a perfect surface was traveling and/or vibrating. Especially, in the Reference [3], the perfect surface was traveling at extremely high velocity, 90% of the light speed. In addition, MOC provides reasonable trends on the following cases: the effects of medium conductivity on the propagation of EM pulse onto conducting dielectric half space [4] and the propagation of EM pulse through lossless non-uniform dielectric slab [5]. To overcome the difficulty stemmed from the rotating cylinder, thanks to the nature of MOC positioning all the field components in center of the grid cell, the PCSBG technique was proposed in coalition with MOC [6, 7]. MOC with the aid of PCSBG was demonstrated to yield reasonable computational results in the scattered EM fields from rotating circular cylinder under the illumination of Gaussian EM pulse [8].

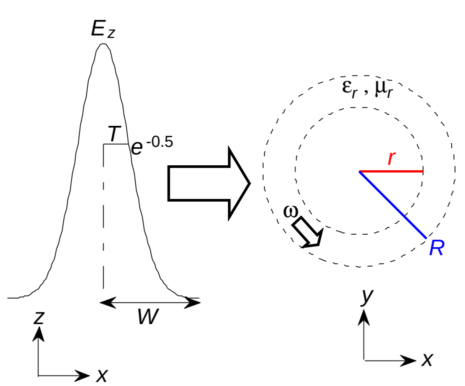

Figure 1: Definition of problem.

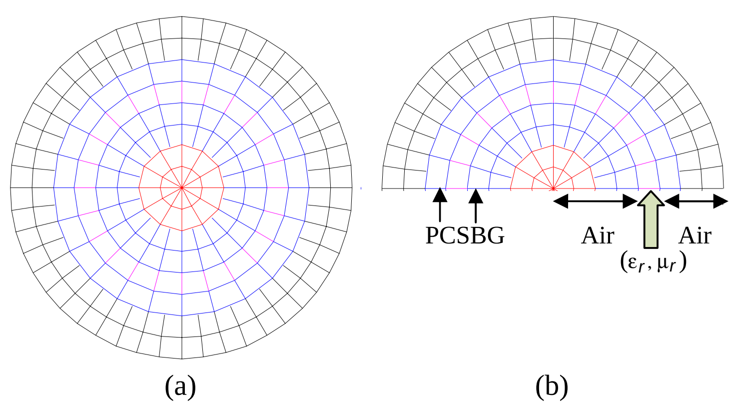

Figure 2: Modified O-type grid system.

2. THE PROBLEM AND THE PASSING CENTER SWING BACK GRIDS

The schematic diagram in Figure 1 depicts the definition of problem. The electric field intensity has a Gaussian profile with a peak value of unity, a width of $T = 0.2\,\text{ns}$ measured from the center to the point of value of $e^{-0.5}$, and a cut-off level at 100 dB for practical reasons. The hollow cylinder is characterized by two radii r and R, the relative permittivity (ε_r) and permeability (μ_r), and the angular velocity ω (counter-clockwise). The EM scattering problems require a minimum quantity on the grid density. A regular O-type grid fails to meet such standard in long radius regions. The modified O-type grid was proposed to settle the situation and a simplified version of which is given in Figure 2(a) where the grid number circumferentially is doubled from zone to zone. Figure 2(b) illustrates the two passing center swing back grids (PCSBGs) layers as well as the definition of the materials that hollow cylinder is made of by giving ε_r and μ_r. Note that both PCSBG layers are portions of air inside and outside of the cylinder and that during the process only grids representing the rotating hollow cylinder and the two PCSBG layers are dynamic while the rest of grids stationary.

Figure 3(a) displays the situation without any treatment two layers of grids immediately adjacent to cylinder's boundaries are badly twisted and suffer from deformation as the hollow cylinder rotates, in which a black arrow indicates the direction of rotation. In Figures 3(b) and 3(c) a dark bold line inside the hollow cylinder and two arrows in PCSBGs are used as indicators. PCSBG is proposed to manipulate all skew grid lines to swing backward by one grid as in Figure 3(c) and then resume the rotation. With the aid of PCSBGs, MOC overcomes the difficulty caused by the rotating object.

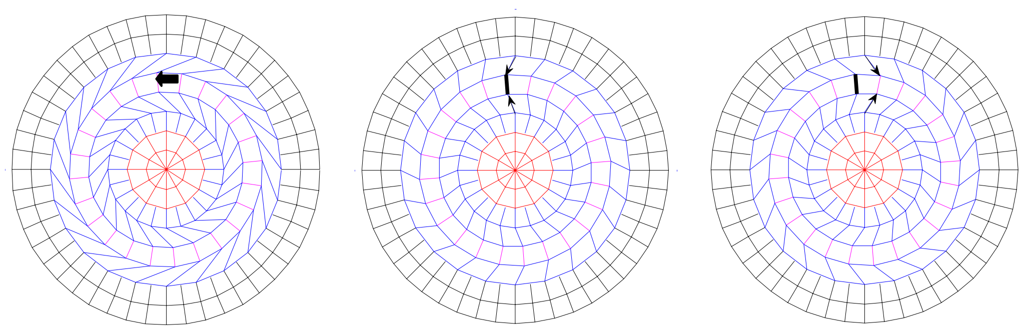

Figure 3: PCSBG in a modified grid: (a) without swing back grids; (b) grid lines pass the center point and are set to swing back; (c) after the swing back rotation continues.

3. THE PROBLEM SET UP

The present problem is featured by a circular hollow dielectric cylinder rotating at extremely high angular frequency which is impractical for the purpose of clear demonstrations the effects of rotating hollow cylinder (either $\varepsilon_r = 4$, $\mu_r = 1$ or $\varepsilon_r = \mu_r = 2$) on the propagation of the EM fields. The dimensions of the numerical model are: $r = 36$ mm, $R = 60$ mm, and domain boundary is 500 mm. The angular frequency ω is set based on the span of time of the Gaussian envelop, i.e., $2W$ in Figure 1. For a pulse width $T = 0.2$ ns, $2W$ is about 1.92 ns with a cut-off level of 100 dB. If the cylinder rotates one tenth of one cycle within $2W$, the instantaneous velocity of any point on the outer surface of the cylinder is about 6.54% of light speed.

The grid density in the unit of points per meter is 250 uniformly in radial direction and ranges from 210 to 680 in circumferential direction (the origin not included). The whole computational domain is composed of three sections. There are three zones in each section: inside (16, 32, 64), interior (64, 128, 256), and exterior (256, 512, 1024) of the hollow cylinder. The three numbers given within parentheses are the grid numbers in each layer from zone to zone. In total, numbers of layer and grid are 144 and 88000, respectively.

4. NUMERICAL RESULTS

Figure 4 illustrates the electric field intensity (E_z) distribution plots for hollow cylinder of $\varepsilon_r = 4$ and $\mu_r = 1$, respectively sampled at 1.033 and 1.833 ns for three different angular frequencies of 0.1 and 0.5. Similar set of plots is given in Figure 5 for cylinder made of impedance matching material ($\varepsilon_r = \mu_r = 2$). A number is given below each plot to indicate the angle degrees that the cylinder rotates at the sampling time. It is obvious that the reflected EM fields can be observed in the second and third rows of Figure 4 while they are undetectable in Figure 5 since the latter

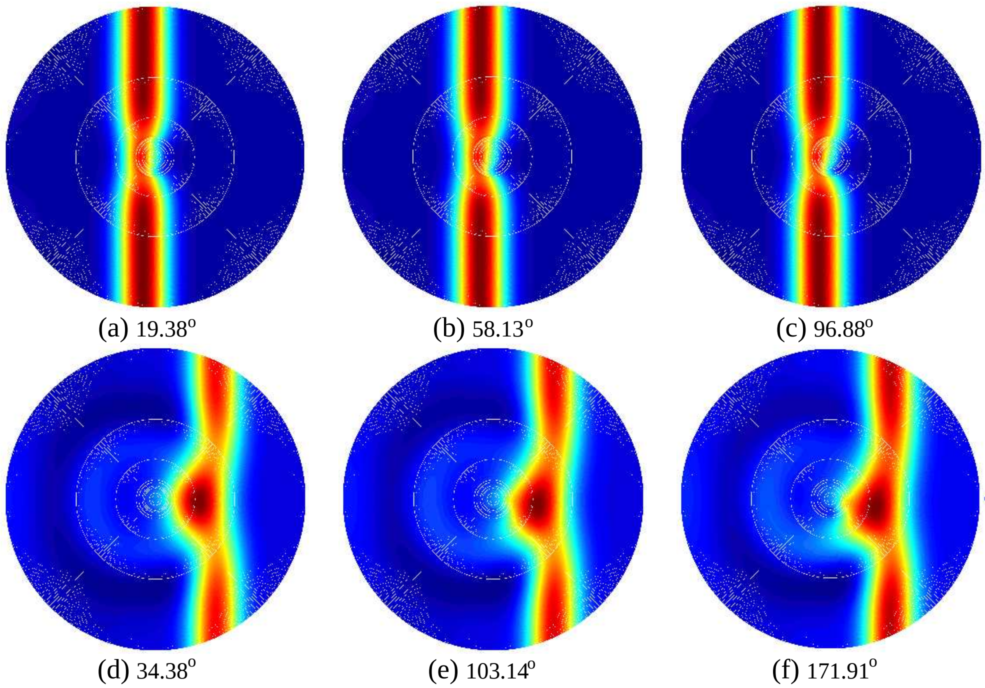

Figure 4: Electric field (E_z) distributions for cylinder ($\varepsilon_r = 4$, $\mu_r = 1$) rotating at three different angular frequencies of (a), (d) 0.1, (b), (e) 0.3, and (c), (f) 0.5 sampled at (a), (b) (c) 1.033 and (d), (e) (f) 1.833 ns.

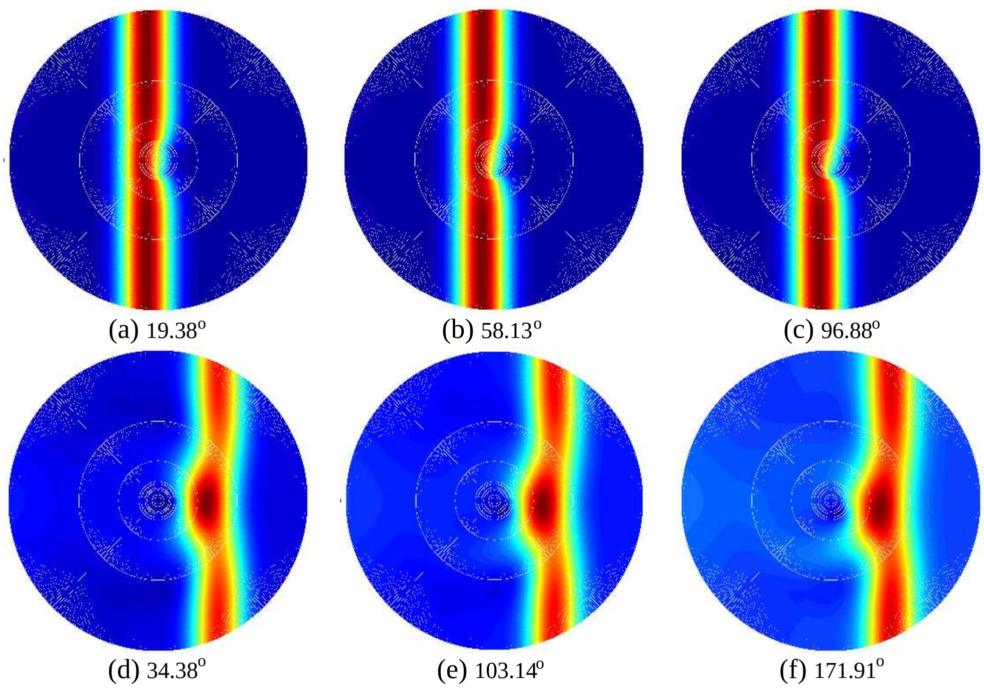

Figure 5: Electric field (E_z) distributions of cylinder ($\varepsilon_r = \mu_r = 2$) rotating at three different angular frequencies of (a), (d) 0.1, (b), (e) 0.3, and (c), (f) 0.5 sampled at (a), (b) (c) 1.033 and (d), (e) (f) 1.833 ns.

is made of impedance matching material. The effects of the rotating hollow cylinder on the EM fields is noticeable, as speed increases the fields are dragged towards lower right for the following reasons: EM fields propagate at slower speed interior of cylinder than in air, and consequently stay in hollow cylinder for a longer time; the EM fields in the lower portion of cylinder propagate in the same direction as the cylinder while the upper opposite, which is getting more perceptible as speed increases.

There is no magnetic field component (solid lines) along the x-axis passing the cylinder center as

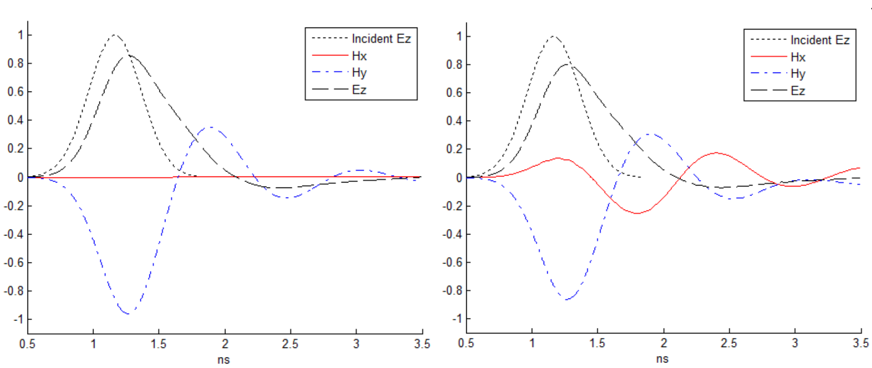

(a) (b)

Figure 6: EM fields recorded at the cylinder ($\varepsilon_r = 4$, $\mu_r = 1$) center: (a) $\omega = 0$, (b) $\omega = 0.3$.

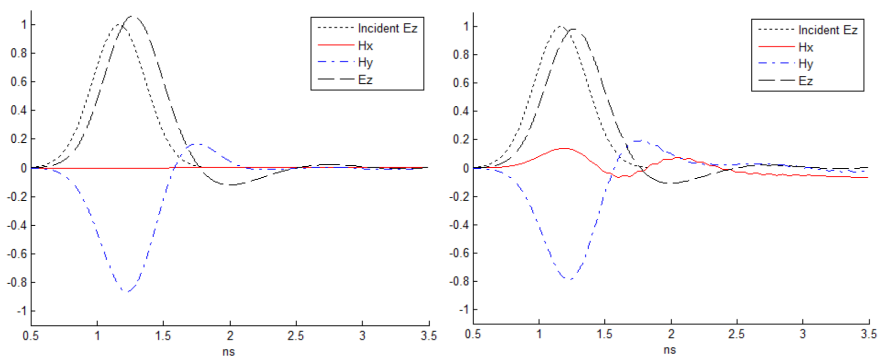

(a) (b)

Figure 7: EM fields recorded at the cylinder ($\varepsilon_r = \mu_r = 2$) center: (a) $\omega = 0$, (b) $\omega = 0.3$.

in Figures 6(a) and 7(a). In both sets of graphs the incident electric field components (dotted lines) are given as a reference. Given in Figures 6(b) and 7(b), it is apparent that x-components of the magnetic fields (H_x) are no longer null in magnitude due to the rotation of the hollow cylinder and fluctuate with greater magnitudes in the dielectric cylinder than that in the impedance matching one. The larger level of fluctuation is originated from the facts that EM fields seem to be trapped interior of the dielectric vessel due to slower in speed and multiple reflection/transmission between interfaces while in the impedance matching vessel such phenomena are barely detectable.

5. CONCLUSION

In this paper, it has been shown that the method of characteristics integrating with the passing center swing back grids technique and solving the time-domain Maxwell equations in the modified O-type grid system, which not only overcame the difficulty of grid distortion due to the rotation of the object of interest but also met the criterion of minimum grid points within the shortest wavelength content. Furthermore, it produced computational outcomes bearing feasible trends of how the rotation of hollow cylinder affects the EM fields by demonstrating the field distribution over the numerical domain and the EM fields sampled at the cylinder center.

REFERENCES

1. Donohoe, J. P., J. H. Beggs, and M. Ho, "Comparison of finite-difference time-domain results for scattered EM fields: Yee algorithm vs. a characteristic based algorithm," *27th IEEE Southeastern Symposium on System Theory*, March 1995.
2. Ho, M., "Scattering of EM waves from traveling and/or vibrating perfect surface: Numerical simulation," *IEEE Transactions on Antennas and Propagation*, Vol. 54, No. 1, 152–156, January 2006.
3. Ho, M., "EM scattering from PEC plane moving at extremely high speed: Simulation in one dimension," *Journal of Applied Science and Engineering (JASE)*, Vol. 17, No. 4, 429–436, December 2014.

4. Ho, M. and F.-S. Lai, "Effects of medium conductivity on electromagnetic pulse propagation onto dielectric half space: One-dimensional simulation using characteristic-based method," *Journal of ElectroMagnetic Waves and Applications*, Vol. 21, No. 13, 1773–1785, 2007.
5. Ho, M., F.-S. Lai, S.-W. Tan, and P.-W. Chen, "Numerical simulation of propagation of EM pulse through lossless non-uniform dielectric slab using characteristic-based method," *Progress In Electromagnetics Research*, Vol. 81, 197–212, 2008.
6. Ho, M., "Simulation of scattered fields from rotating cylinder in 2D: Under illumination of TE and TM Gaussian pulses," *PIERS Proceedings*, 1646–1651, Moscow, Russia, August 18–21, 2009.
7. Ho, M., "Numerically solving scattered electromagnetic fields from rotating objects using passing center swing back grid technique: A proposal," *Journal of ElectroMagnetic Waves and Applications*, Vol. 23, No. 23, 389–394, 2009.
8. Ho, M., "Simulation of scattered EM fields from rotating cylinder using passing center swing back grids technique in two dimensions," *Progress In Electromagnetics Research*, Vol. 92, 79–90, 2009.